Electronic structure of Co-Pt alloys: X-ray spectroscopy and density-functional calculations

Y. S. Lee
Division of Information Communication & Computer Engineering and Institute of Semiconductor Technology, Hanbat National University, Daejon 305-719, Korea

J. Y. Rhee
Department of Physics, Hosea University, Asan, Choongnam, 336-795, Korea

C. N. Whang
ASSRC and Department of Physics, Yonsei University, Seoul 120-749, Korea

Y. P. Lee
Quantum Photonic Science Research Center and Department of Physics, Hanyang University, Seoul 133-791, Korea
(Received 22 May 2003; revised manuscript received 16 September 2003; published 18 December 2003)

The K and $L_{2,3}$ absorption edges and core-level binding-energy shifts for pure Co and Pt, and Co-Pt alloys are measured to investigate the changes in electronic structures of Co-Pt alloys. The results agree well with those of the first-principles calculations of the electronic structures by using a full-potential linearized-augmented-plane-wave method. It is found that there is an enhancement of the hybridization between the Co $3d$ and Pt $5d$ orbitals upon alloying. Consequently, as the Pt concentration increases, both Pt and Co gains d electrons, and there is a concomitant decrease in s and p electrons at both sites. This enhanced hybridization in the alloy leads to a net charge transfer from the Co to Pt site in accordance with the predictions based on the electronegativity. For the core-level shifts in Co-Pt alloys the initial-state effects are more important to the Pt $4f$ level, while the relaxation effects play a more important role for the Co $2p$ level.

DOI: 10.1103/PhysRevB.68.235111 PACS number(s): 78.70.Dm, 79.60.−i, 71.20.−b

I. INTRODUCTION

Co-Pt alloys, which are composed of a ferromagnetic $3d$ transition metal and paramagnetic $5d$ element, have attracted much interest because of their high chemical stability and large magnetic anisotropy. When Co and Pt form binary alloys, ordered crystalline phases are possible at three stoichiometric compositions, i.e., Co_xPt_{1-x} with $x=0.25$, 0.5, and 0.75; cubic $L1_2$ type for $x=0.25$ and 0.75, and tetragonal $L1_0$ type for $x=0.5$. The chemical ordering and magnetic properties of the Co-Pt alloy systems have been extensively studied.[1–4] Recently, it was found that ion-beam mixing of Co/Pt multilayered film under an external magnetic field led to the formation of a metastable phase with a measured magnetic moment per Co atom of $2.63\mu_B$, which is one of the highest values ever observed in the ferromagnetic bulk phase.[5] Since the magnetic properties are closely related to the electronic structures, there are several first-principles *ab initio* calculations of the electronic structures of these alloy systems.[6–9] Kootte *et al.*[8] calculated the spin-polarized band structures of Co_xPt_{1-x} alloys with $x=0$, 0.25, 0.5, 0.75, and 1, and the results were used to deduce various ground-state properties such as the total and spin- and angular-momentum-decomposed density of states (DOS), magnetic moments, charge transfers, and so on. The calculated magnetic moments are in good agreement with experiments, and the moments of the Co atoms and the induced moments of the Pt atoms do not vary significantly with x. It was also shown that there were strong indirect exchange interactions between Co magnetic moments via one intermediate Pt atom, as well as direct Co-Co interactions between the nearest and next-nearest neighbors.

However, the experimental study of the electronic structures of Co-Pt alloys has been performed to a less extent. From the results of the spin-polarized band-structure calculations, it is generally accepted that there is a small charge transfer from Co to Pt in the alloys.[6–8] On the other hand, in order to understand various effects of the electronic charge distribution of the Co_xPt_{1-x} alloys with different x's in detail, it is desirable to investigate the electronic structures experimentally as well as theoretically.

To study the electronic structure changes and, as a result, the charge redistribution between Co and Pt in the Co-Pt alloy systems, we employed x-ray-absorption spectroscopy (XAS) and x-ray photoelectron spectroscopy (XPS) techniques which provide a better understanding of the electronic structures and the charge distribution of the specimen. The interpretation of the experimental results was further supported by the theoretical electronic structure calculations by using a full-potential linearized-augmented-plane-wave (FPLAPW) method. As a preliminary result of this work, changes in the Pt $5d_{5/2}$ and Co $4p$ states of Co-Pt alloys have been briefly published elsewhere.[10] This paper is organized as follows; the experimental procedures and theoretical details are presented in Secs. II and III, respectively, the results and discussion are given in Sec. IV, and the paper is concluded in Sec. V.

II. SAMPLE PREPARATION AND EXPERIMENTAL PROCEDURES

Bulk Co_xPt_{1-x} alloy samples with $x=0.25$, 0.5, and 0.75 were prepared by comelting. X-ray diffraction (XRD) was

TABLE I. Parameters used in the FPLAPW calculations. The last column (V_{MT}/V_{cell}) is the fraction of volume occupied by the MT spheres. "N/A" stands for "not applicable."

	Space group	a (a.u.)	c (a.u.)	vol./atom $(\text{a.u.})^3$	R_{MT}^{Co} (a.u.)	R_{MT}^{Pt} (a.u.)	V_{MT}/V_{cell} (%)
α-Co	$P6_3/mmc$	4.7377	7.6885	74.73	2.354	N/A	73.6
Co_3Pt	$Pm3m$	6.9232	N/A	82.96	2.415	2.481	72.6
CoPt	$P4/mmm$	5.0817	6.9939	90.30	2.473	2.541	73.1
$CoPt_3$	$Pm3m$	7.2830	N/A	96.57	2.506	2.575	73.9
Pt	$Fm3m$	7.4136	N/A	101.87	N/A	2.621	74.1

carried out for the structural analysis. The crystal structures of samples were confirmed to be ordered phases; $AuCu_3$ type ($L1_2$ phase) for $x=0.25$, AuCu type ($L1_0$ phase) for $x=0.5$, and $AuCu_3$ type ($L1_2$ phase) for $x=0.75$. Co K- and Pt $L_{2,3}$-edge x-ray-absorption near-edge spectroscopy (XANES) spectra were obtained at the 3C1 EXAFS beam line in the Pohang Accelerator Laboratory.

For XPS, $2p$ and $4f$ core-level spectra of the alloys were taken in PHI 5700 ESCA system. Each sample was cleaned *in situ* by Ar^+ ion bombardment to remove contaminated surface layers. The sputtering was done with the 3 keV Ar^+ ion beam (current $\sim 1\ \mu$A) in a pressure of 3×10^{-7} Torr. After the Ar-ion sputtering of the sample surface, the composition of the surface layers might be different from that of the bulk. However, since this alloy does not belong to the surface-segregation system,[11] the error due to segregation, if any, would be very small. We thus used the bulk values for the alloy concentrations. The other experimental details are given in Ref. 10.

III. ELECTRONIC STRUCTURE CALCULATIONS

The electronic band structures of Co_xPt_{1-x} ($x=0$, 0.25, 0.5, 0.75, and 1) alloys were calculated using a FPLAPW method[12] within the generalized-gradient approximation (GGA). All the calculations were spin-polarized ones with the spin-orbit interactions included in the self-consistent iterations. For the case of pure Pt we also performed the spin-polarized calculations to ensure the consistency with other alloys and pure Co. For the exchange-correlation effects we used a GGA version of Perdew, Burke, and Ernzerhof.[13] Following bands are treated as valence: Co $3p$, $3d$, $4s$, and $4p$, and Pt $5p$, $5d$, $6s$, and $6p$. The atomic core density and, hence, the core levels were calculated fully relativistically at each iteration. We used the experimental lattice constants. The muffin-tin (MT) radii of the atomic spheres are determined in such a way that all the spheres are almost in contact for the pure Co and Pt metals and equiatomic CoPt alloy. The MT sphere of Co (Pt) atoms are also almost in contact for Co_3Pt ($CoPt_3$) alloy. In the case of equiatomic CoPt alloy ($L1_0$ phase) they are naturally determined to satisfy the relationship, $R_{MT}^{Pt}/R_{MT}^{Co}=1.0275$, where R_{MT}^{X} is the MT radius of atom X ($X=$Co or Pt). We used this ratio for the determination of R_{MT}^{Co} and R_{MT}^{Pt} for Co_3Pt and $CoPt_3$, respectively. The parameters used in the calculations are summarized in Table I. To calculate the Pt $4f$ and Co $2p$ core-level shift (CLS) we employed a single-cell model by introducing a fractional number of core hole.[14] This approximation is known as the "Slater's Transition State."[15] The numbers of inequivalent **k** points in the irreducible wedge of the primitive reciprocal unit cell for the self-consistent-field calculations are 392 for α-Co, 528 for CoPt, 405 for Pt, and 288 for Co_3Pt and $CoPt_3$. These large numbers of **k** points are necessary to ensure the convergence of the Kohn-Sham eigenvalues for accurate core-level calculations. For the calculations of the DOS an improved linear-energy-tetrahedron method[16] with a finer mesh of irreducible wedge was employed.

IV. RESULTS AND DISCUSSION

Figure 1 shows the Co K-edge absorption spectra for pure Co and Co-Pt alloys. These spectra were background subtracted by fitting the preedge background using the least-square method. The spectra were then normalized with the multiplication by a factor which makes the continuum step equal to unity at the higher energy region.

When the Pt content increases, peaks denoted as a and b in Fig. 1 exhibit a change in strength. The variation of the peak strengths can be discussed in terms of the charge redis-

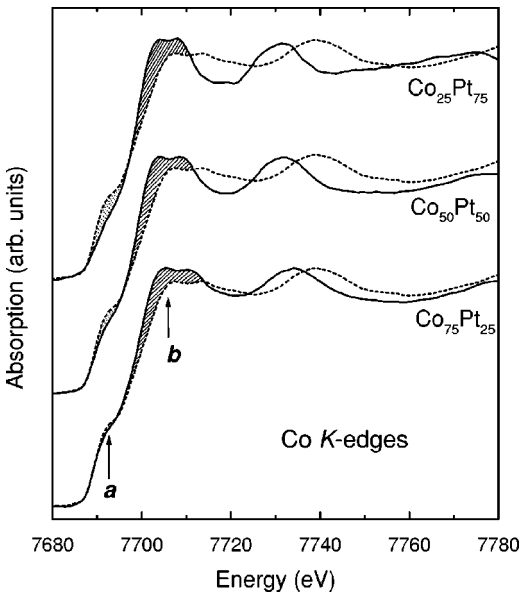

FIG. 1. Co K absorption edges of Co_xPt_{1-x} alloys (solid lines) and pure Co (dashed lines).

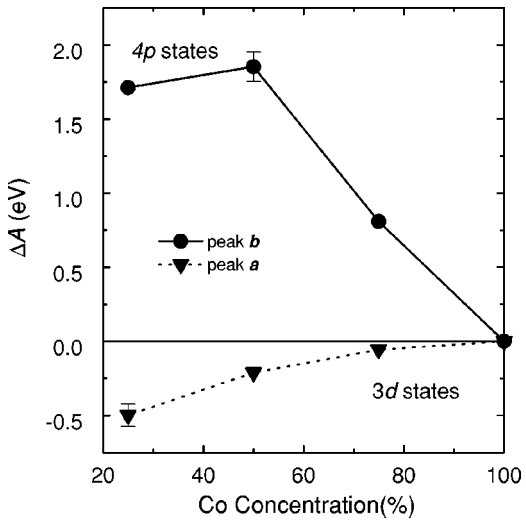

FIG. 2. Variation of the areas of the Co *K*-edge peak *a* and *b* in Fig. 1 as a function of the Co concentration.

tribution between Co and Pt atoms in alloy. The evolution of the threshold peak *a* upon alloying mainly reflects the change of the $3d$ character of unoccupied states.[10,17,18] Therefore, we could obtain some information for the change of Co $3d$ states from the peak *a* of Co *K*-edge spectrum indirectly even though it would be more evident if the change of Co $3d$ states in alloy was estimated from the Co $L_{2,3}$ absorption-edge spectra, which reflect the direct $2p \rightarrow 3d$ dipole transition. In addition, the evolution of the main peak *b* reflects the change of the $4p$ character of the unoccupied states.[10] These peaks are sensitive to an alteration in the DOS upon alloying.[19] The variation of the peak areas $\Delta\mathcal{A}$ is presented in Fig. 2 as a function of the Co concentration. The $\Delta\mathcal{A}$'s were calculated by integrating the difference spectra in an appropriate energy range (cross-hatched areas of Fig. 1). The difference spectrum is the difference between the spectrum of the respective alloy and that of elemental Co. Therefore, $\Delta\mathcal{A}$ could be either positive, when the absorption is stronger in alloy than in elemental Co, or negative, if the situation is reversed.

As shown in Figs. 1 and 2, $\Delta\mathcal{A}$ of the main peak *b* increases as the Pt concentration increases. This means that the number of occupied states of the Co $4p$ electrons decreases upon alloying. On the other hand, $\Delta\mathcal{A}$ of peak *a* is reduced (becomes more negative) as the Pt concentration increases, implying that the Co $3d$ states are filled upon alloying. This interpretation will be further discussed in conjunction with the results of the FPLAPW calculations. The absorption cross section in the *K*-edge spectra of transition metals are strongly influenced by the *p*-*d* hybridization due to the unoccupied *d* bands; in the system with a weak *p*-*d* hybridization, the *p*-like DOS is strongly reduced and the *K*-edge threshold is depressed.[20] Therefore we ascribe the reduction of the Co $4p$ states and the depression of peak *a* to the weakened *p*-*d* hybridization at the Co sites upon alloying.

Figures 3 and 4 show the Pt L_2- and L_3-edge absorption spectra, respectively, obtained for pure Pt and Co-Pt alloys. These spectra were also normalized in a similar way to the

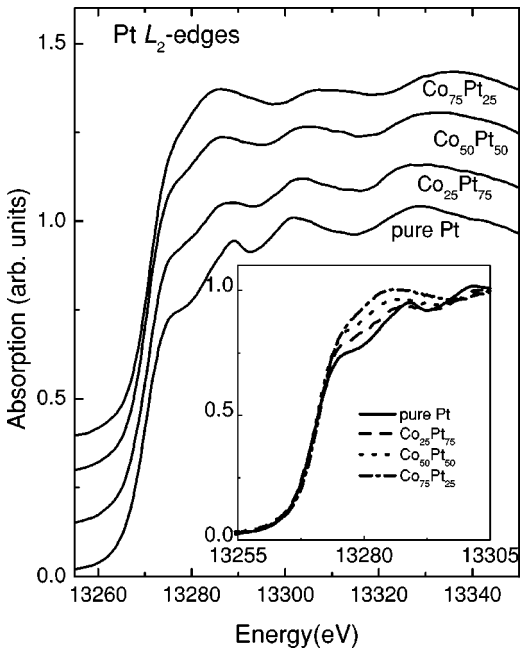

FIG. 3. X-ray-absorption spectra for Pt L_2-edge of pure Pt and Co-Pt alloys.

case of the Co *K*-edge spectra. In pure Pt, the L_2-edge white line (WL) is absent as in the L_3 edge of pure Ag.[21] Since the Pt L_2-edge spectrum is governed mainly by the $2p_{1/2} \rightarrow 5d_{3/2}$ transitions and no $2p_{1/2} \rightarrow 5d_{5/2}$ transitions are allowed based on the selection rules, the absence of WL indicates that there is no $5d_{3/2}$ hole in pure Pt.[22] Upon alloying, the strength of the Pt L_2 WL feature is built up with respect to pure Pt, as shown more clearly in the inset of Fig. 3.

On the other hand, the Pt L_3-edge absorption spectra in Fig. 4 are quite different from those of the Pt L_2 edge. In Fig. 4, the zero of energy is assigned to the WL maximum point of each spectrum because the WL maximum corresponds to the Fermi level E_F of pure Pt, where the unoccupied final $5d$

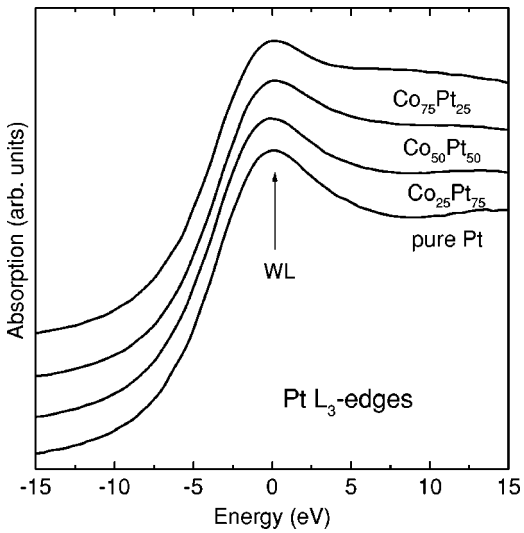

FIG. 4. X-ray-absorption spectra for Pt L_3 edge of pure Pt and Co-Pt alloys.

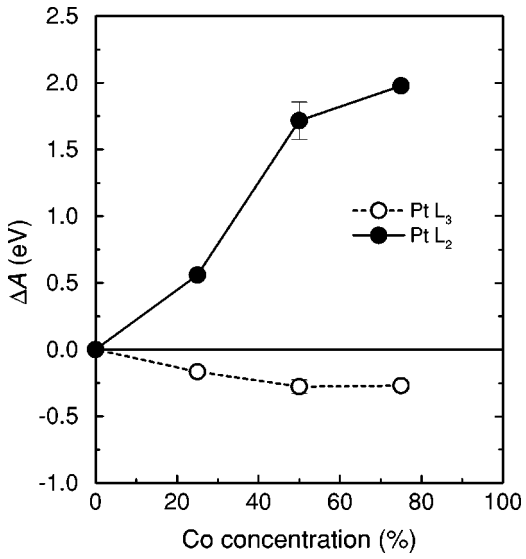

FIG. 5. $\Delta\mathcal{A}$ of the Pt $L_{2,3}$-edges WL as a function of the Co concentration.

states have a narrow bandwidth.[20] As shown in Fig. 4, the strength of the Pt L_3-edge WL feature is reduced drastically compared to that of pure Pt as the Co concentration increases. Although the L_3 near-edge spectrum probes the $2p_{3/2} \rightarrow 5d_{3/2,5/2}$ dipole transitions, the Pt L_3 near-edge spectrum includes only the unoccupied $d_{5/2}$ character,[23] owing to the absence of the Pt L_2-edge WL, that is, the nonexistence of the $5d_{3/2}$ holes in pure Pt. Therefore, the reduction of the Pt L_3-edge WL strength indicates that the unoccupied $d_{5/2}$ DOS projected onto the Pt atomic sphere is diminished as the Co concentration increases upon alloying. In addition, since the strength reduction means that the hybridization of the d states becomes stronger, the decreasing Pt L_3 WL area in Co-Pt alloys reflects the fact that the Pt-sphere-projected Co-Pt hybridized d states increases. This result agrees well with our calculated results below, as well as those of Kootte *et al.*[8] In Ref. 8, it was concluded that there is a very strong hybridization between the Co $3d$ and Pt $5d$ orbitals by analyzing the results of the *ab initio* spin-polarized band-structure calculations.

To understand better the change in $5d$ state at the Pt sites, $\Delta\mathcal{A}$ of WL, defined in the same way as for the Co K-edge absorption spectra, is shown in Fig. 5 as a function of the Co concentration. It is very interesting that $\Delta\mathcal{A}$'s of the Pt L_2- and L_3-edge WL have opposite signs. For the Pd L_2- and L_3-edge WL of Pd-Ag alloys the signs are identical.[21] In spite of the opposite signs, the absolute magnitudes decrease as the Pt concentration increases, and that of the Pt L_2 WL is relatively larger. This may indicate that the number of Pt $5d$ empty states increases as the Co concentration increases, and, considering the opposite signs, we can conclude that the $5d_{3/2}$ states are depleted and the $5d_{5/2}$ states are filled at the Pt sites upon alloying.

From the above experimental results, we can find a charge redistribution in Co-Pt alloys; the occupied Co $4p$ DOS decreases and the occupied Pt $5d$ and Co $3d$ DOS increases as the Pt concentration increases. However, one should be very cautious in interpreting the charge redistribution correctly. As shown in Figs. 2 and 5, the sign of $\Delta\mathcal{A}$ for the Co $4p$ ($3d$) electron is positive (negative), and that of the sum of $\Delta\mathcal{A}$'s for the Pt L_2- and L_3-edge WL is positive. It implies that, upon alloying, Pt loses a fraction of its $5d$ electrons with respect to elemental Pt, while Co gains $3d$ electrons with a concomitant decrease in p electrons with respect to elemental Co. Nevertheless, without the results of electronic structure calculations, we are not able to know about the net charge transfer between Co and Pt sites upon alloying in detail. Therefore, we performed the electronic structure calculations using a FPLAPW method as aforementioned and presented

TABLE II. Angular-momentum decomposed electron numbers in each atomic sphere of Co-Pt alloys. Q_{MT} is the total charge inside the MT spheres. The interstitial charge "INT" is the difference between the total charge, obtained by the "AIM" method described in the text, and Q_{MT}. $\triangle Q_{\mathrm{TOT}}$ is the amount of total charge transfer. N/A stands for not applicable.

Atom		α-Co	Co_3Pt	CoPt	$CoPt_3$	Pt
Co	$3d$	7.2279	7.2768	7.3323	7.3612	N/A
	$4s$	0.4694	0.4714	0.4723	0.4543	N/A
	$4p$	0.4747	0.5009	0.5225	0.5120	N/A
	$4f$	0.0353	0.0448	0.0548	0.0578	N/A
	INT	0.7805	0.4851	0.2584	0.1163	N/A
	Q_{MT}	8.2194	8.3113	8.4017	8.4068	N/A
	$\triangle Q_{\mathrm{TOT}}$	0.0000	−0.1991	−0.3383	−0.4685	N/A
Pt	$5d$	N/A	7.4947	7.6176	7.6901	7.7918
	$6s$	N/A	0.5779	0.5839	0.5755	0.5715
	$6p$	N/A	0.4362	0.4747	0.4917	0.5124
	$5f$	N/A	0.0523	0.0648	0.0766	0.0897
	INT	N/A	1.9999	1.5797	1.3176	1.0052
	Q_{MT}	N/A	8.5753	8.7614	8.8587	8.9948
	$\triangle Q_{\mathrm{TOT}}$	N/A	0.5972	0.3383	0.1562	0.0000

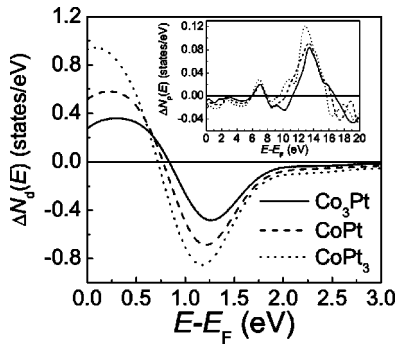

FIG. 6. Differences in Co d DOS between $Co_{1-x}Pt_x$ alloys and pure Co. $\Delta N_d(E) \equiv N_d^{Co_{1-x}Pt_x}(E) - N_d^{Co}(E)$. Inset shows the differences in Co p DOS.

various information obtained from the calculations in Table II.

Table II summarizes the angular-momentum-decomposed electron numbers in each atomic sphere. The difference between Q_{MT} and the sum of s, p, d, and f components is the electron number with the angular momentum higher than $l=3$. The topology of the electron density was analyzed according to Bader's ''atom-in-molecule (AIM)'' theory[24] to get the ''total'' charge. Although there is no consensus for the method to calculate the total charge belongs to a particular atom in an alloy, the AIM theory can be considered to be a reasonable choice for defining the real total charge that belongs to the respective atom.

It is noticed that the theoretical results confirm the interpretations of the experimental results by XANES, i.e., both the Co $3d$ and Pt $5d$ states are filled as the Co concentration decreases. The number of $4p$ electrons inside the Co MT sphere, however, increases as the Co concentration decreases. Although this tendency of the calculational results seems to be opposite to the experimental results, one can see that the Co $4p$ states are also in accordance with the experimental results, if the charges in the interstitial region are properly taken into account. Since the d electrons are fairly well localized, the charges in the interstitial region must be mostly s and p characters. Assuming that the ratio of s electrons to p electrons in the interstitial region is the same as that in the MT sphere, the number of $4p$ electrons belonging to the Co atom decreases as the Co concentration decreases, confirming the experimental results. This electron redistribution in the alloy leads to a net charge transfer from the Co to Pt sites (see rows designated as Q_{TOT} in Table II). The calculated net charge transfers to the Pt site in Co-Pt alloys satisfies the electronegativity requirement, and are quite similar to the results of Ref. 8.

Both the DOS effects and the transition-matrix-element effects should be taken into account in the interpretation of the XAS spectra. Since we have considered only the DOS effects in our interpretation of the XAS data, one may suspect our interpretation. In order to wipe out this skepticism, we have analyzed the angular momentum and site decomposed DOS. Figure 6 shows the differences in the unoccupied Co d DOS between $Co_{1-x}Pt_x$ alloys and pure Co. We applied the Gaussian broadening to the DOS curves with the lifetime of 0.3 eV. In the 0.7–2.0 eV energy range above E_F, which corresponds to the peak a in Fig. 1, the Co d-DOS decreases as the Pt concentration increases. This decrease is due to the movement of the minority-spin Co d bands located at ~ 1.2 eV above E_F in pure Co toward E_F, indicating an increase of the Co d-electron occupation upon alloying with Pt. In this region the unoccupied Co p DOS also decreases as the Pt concentration increases (see the inset of Fig. 6), while it increases in the 11–16 eV energy range, corresponding to the peak b in Fig. 1. Since it is hardly believable that the wave functions of the Co d electron change significantly upon alloying, the transition-matrix-element effects are not very important at least for the change in the XAS spectra upon alloying. Therefore, we can safely conclude that the change in the XAS spectra upon alloying is predominantly determined by the change in DOS.

Generally, it is well known that the changes in valence state are dominantly determined by the hybridization between neighboring atoms upon alloying, leading to CLS.[25] According to Ref. 26, CLS occurs as a result of E_F shift, atomic volume change, squeezing of valence electrons, core $\leftrightarrow$valence repulsion, screening effects, and so on. For the simplicity, we can categorize all these effects into the initial- and final-state effects. The initial-state effects can be mostly determined by the interatomic charge transfer and the intra-atomic charge redistributions. The intra-atomic charge redistribution is sometimes called as the configuration change.The Pt $4f$ and Co $2p$ CLS's measured by XPS are given as $\triangle\mathcal{B}_{exp}$ rows in Table III.

As shown in Table III, the Pt $4f_{7/2}$ and Co $2p_{3/2}$ XPS core levels shift toward the higher and lower binding energy in alloys, respectively. These observed CLS are opposite to the prediction of the general rule.[26] If an atom loses a part of its electronic charge, the core levels in general deepen, i.e., the binding energy increases. Since the positive nuclear charge does not change, while the valence electronic charge decreases, the remnant electrons feel stronger attraction, resulting in increased binding energies of core levels. Since Pt is more electronegative than Co (2.2 for Pt and 1.8 for Co in Pauling's value[27]), one would expect that the Pt core levels shift toward the lower energy, resulting in $\triangle\mathcal{B}_{expt}$ for Pt negative. For the Co atoms the argument is reversed. Although the measured $\triangle\mathcal{B}_{expt}$'s for Pt and Co are positive and negative in alloys, respectively, the sign of the respective values of $\triangle\mathcal{B}_{expt}$ seem to be opposite to the tendency expected by the general rule. One should note that, however, these arguments can only be applied to the initial-state effects to CLS.

It is notorious that the local-density-approximation calculations of core-level binding energy does not properly reproduce the experimental results, such as XPS. The final-state effects, or relaxation effects, should be considered in analyzing CLS. However, we can treat the difference between the Kohn-Sham eigenvalues of elemental metal and alloy as the initial-state effect to CLS.[28] These results are summarized in Table III as $\triangle\mathcal{B}_i$. $\triangle\mathcal{B}_i$ is defined as

$$\triangle\mathcal{B}_i \equiv (E_F^{alloy} - E_{core}^{alloy}) - (E_F^{pure} - E_{core}^{pure}), \qquad (1)$$

TABLE III. Core-level binding energy shifts ($\triangle\mathcal{B}_{\mathrm{exp}}$ [eV]) for Pt $4f_{7/2}$ and Co $2p_{3/2}$ obtained from the XPS measurements and the calculations. The subscripts "expt," "i," and "r" stand for experimental value, initial-state effect, and final-state or relaxation effect, respectively, and $\triangle Q_{\mathrm{p}}$ is the fractional number of electronic charge promoted to the valence from the respective core level to represent the partial core-hole effects (see text). All the values are determined relative to the corresponding elemental metal.

Atom		α-Co	Co_3Pt	CoPt	$CoPt_3$	Pt
Co	$\triangle\mathcal{B}_{\mathrm{expt}}$		-0.08	-0.19	-0.19	N/A
	$\triangle\mathcal{B}_{\mathrm{i}}$		0.10	0.09	0.05	N/A
	$\triangle\mathcal{B}_{\mathrm{r}}$		-0.18	-0.28	-0.24	N/A
	$\triangle Q_{\mathrm{p}}$	0.518	0.520	0.518	0.521	N/A
Pt	$\triangle\mathcal{B}_{\mathrm{expt}}$	N/A	0.30	0.25	0.10	
	$\triangle\mathcal{B}_{\mathrm{i}}$	N/A	0.23	0.21	0.20	
	$\triangle\mathcal{B}_{\mathrm{r}}$	N/A	0.07	0.04	-0.10	
	$\triangle Q_{\mathrm{p}}$	N/A	0.535	0.540	0.555	0.585

where E_{core} is the Kohn-Sham eigenvalue of the core level. The difference $\triangle\mathcal{B}_{\mathrm{expt}}-\triangle\mathcal{B}_{\mathrm{i}}$ is the final-state effects to CLS (denoted as $\triangle\mathcal{B}_{\mathrm{r}}$ in Table III).

As was pointed out in Ref. 29, the valence contribution (initial-state effects) to the CLS is mainly governed by the change in *d*-electron occupancy, rather than the total number of electrons or simply *sp*-electron number, in various alloys. It was further confirmed by several other reports.[30] The *d* electrons are more localized than the *s* and *p* electrons, resulting in larger effects on the core electrons, and the valence $\leftrightarrow$core repulsion is larger, owing to the larger angular momentum than the *s* and *p* electrons. This is the case in our samples. With the results of the FPLAPW calculations (see Table II), we can explain the Pt $4f$ and Co $2p$ CLS in Co-Pt alloys. As can be seen in Table III for the Co site $\triangle\mathcal{B}_{\mathrm{i}}$ is positive even though the Co $3d$ occupation number is increasing upon alloying. The magnitudes of $\triangle\mathcal{B}_{\mathrm{i}}$ is very small compare to those of $\triangle\mathcal{B}_{\mathrm{r}}$. Since the Co $2p$ level is quite deep and more localized than Co $3d$ level, the wave-function overlap is small and hence change in Co $3d$ occupation number has little effect on $\triangle\mathcal{B}_{\mathrm{i}}$. Moreover, the variation of Co $3d$ occupation number upon alloying is small (0.14 electrons between pure Co and $CoPt_3$). Therefore, it can be concluded that for the Co site the variation in total number of electrons is more important than that of the Co $3d$ occupation number in determination of the sign and magnitude of $\triangle\mathcal{B}_{\mathrm{r}}$. On the other hand, for the Pt site the magnitude of $\triangle\mathcal{B}_{\mathrm{r}}$ is much larger than that of $\triangle\mathcal{B}_{\mathrm{i}}$. Both experimental and theoretical results indicate a reduced number of *d* electrons at the Pt site upon alloying, resulting in positive $\triangle\mathcal{B}_{\mathrm{i}}$ in Pt atom. Since the amount of the lost $5d$ electrons at the Pt site increases as the Co concentration increases, the magnitude of the Pt $4f$ $\triangle\mathcal{B}_{\mathrm{i}}$ increases. The Pt $4f$ level is not too deep and the wave-function overlap between the Pt $4f$ and $5d$ levels is significant, Hence, the variation in the Pt $5d$ occupation number produces more pronounced effects in determination of $\triangle\mathcal{B}_{\mathrm{i}}$ than that of total number of electrons.

$\triangle\mathcal{B}_{\mathrm{r}}$ is closely related to $\triangle\mathcal{Q}_{\mathrm{p}}$, where $\triangle\mathcal{Q}_{\mathrm{p}}$ is the charge promoted to the valence band from the respective core level. An introduction of partial core hole to the core level enables the Kohn-Sham eigenvalue of the respective core level to be precise reproduction of the experimental core-level binding energy. We treat the fractional number of core-level electrons as the fitting parameter to exactly reproduce the core-level binding energy measured by XPS. $\triangle\mathcal{Q}_{\mathrm{p}}$ is the difference between the number of electrons for fully occupied core level and that of partially filled core level. For the Co site $\triangle\mathcal{Q}_{\mathrm{p}}$ is not sensitive to the Pt concentration. It is consistent with fact that CLS is dominated by the final-state effects for the Co site. For the case of the Pt site the arguments are reversed.

V. CONCLUSIONS

We performed XANES and XPS experiments of Co-Pt alloys to understand their electronic structures. It was found that, in Co-Pt alloys, there was a substantial increase in the area of the Pt L_2 (unoccupied $d_{3/2}$ states) WL and a decrease in that of the Co *K*-edge threshold (peak *a* in Fig. 1) with respect to pure Pt and Co, respectively. From these results, we suggest that the hybridization between the Co $3d$ and Pt $5d$ orbitals is enhanced upon alloying, resulting in a loss in Pt *d* electrons and a gain in Co *d* electrons with respect to the respective elemental metals. The observed shifts of the core-level binding energies by XPS agree well with the XANES results, although they seem to be inconsistent with the general rule of electronegativity. Using the results of the FPLAPW calculations, we have estimated the direction of charge transfer in Co-Pt alloys. The calculations show that there is a decrease in *p*-like conduction electrons and an increase in *d* electrons at the Co site upon alloying, which is in accordance with the experiments. In addition, the calculations reveal that this electron redistribution in the alloy leads to a net charge transfer from the Co to Pt site consistently with the electronegativity rules. The Pt $4f$ and Co $2p$ CLS's in Co-Pt alloys, which are seemingly in disagreement with the electronegativity predictions, can be explained by discriminating the initial- and final-state effects with the aid of FLAPW calculations. For CLS's of Co-Pt alloys the initial-state effects contribute dominantly to the Pt $4f$ CLS, while the final-state or relaxation effects play a more important role for Co $2p$ CLS.

ACKNOWLEDGMENTS

This work was supported by the Korea Science and Engineering Foundation through Quantum Photonic Science Research Center at Hanyang University and through Grant No. R04-2002-000-00009-0, and by a Korea Research Foundation Grant (KRF-2001-015-DP0193).

[1] J.M. Sanchez, J.L. Morán-Lopéz, C. Leroux, and M.C. Cadeville, J. Phys.: Condens. Matter **1**, 491 (1989).
[2] D. Weller, H. Brandle, G. Gorman, C.-J. Lin, and H. Notarys, Appl. Phys. Lett. **61**, 2726 (1992); D. Weller, H. Brandle, and C. Chappert, J. Magn. Magn. Mater. **121**, 461 (1993).
[3] T.A. Tyson, S.D. Conradson, R.F.C. Farrow, and B.A. Jones, Phys. Rev. B **54**, R3702 (1996).
[4] G. Schütz, R. Wienke, W. Wilhelm, W.B. Zeper, H. Ebert, and K. Spörl, J. Appl. Phys. **67**, 4456 (1990).
[5] G.S. Chang, Y.P. Lee, J.Y. Rhee, J. Lee, K. Jeong, and C.N. Whang, Phys. Rev. Lett. **87**, 067208 (2001).
[6] T. Tohyama, Y. Ohta, and M. Shimizu, J. Phys.: Condens. Matter **1**, 1789 (1989).
[7] Y. Ohta, M. Miyauchi, and M. Shimizu, J. Phys.: Condens. Matter **1**, 2637 (1989).
[8] A. Kootte, C. Haas, and R.A. de Groot, J. Phys.: Condens. Matter **3**, 1133 (1991).
[9] G. Moraitis, J.C. Parlebas, and M.A. Khan, J. Phys.: Condens. Matter **8**, 1151 (1996).
[10] Y.S. Lee, Y.D. Chung, K.Y. Lim, C.N. Whang, Y. Jeon, and B.S. Choi, J. Korean Phys. Soc. **35**, S560 (1999).
[11] P.M. Ossi, Surf. Sci. **201**, L519 (1988).
[12] P. Blaha, K. Schwarz, G. K. H. Madsen, D. Kvasnicka, and J. Luitz, *WIEN2k, An Augmented Plane Wave + Local Orbitals Program for Calculating Crystal Properties* (Karlheinz Schwarz, Techn. Universität Wien, Austria, 2001).
[13] J.P. Perdew, K. Burke, and M. Ernzerhof, Phys. Rev. Lett. **77**, 3865 (1996).
[14] J. Luitz, M. Maier, C. Hèbert, P. Schattsschneider, P. Blaha, K. Schwarz, and B. Jouffrey, Eur. Phys. J. B **21**, 363 (2001).
[15] J. C. Slater, *The Self-consistent Field for Molecules and Solids, Quantum Theory of Molecules and Solids* (McGraw-Hill, New York, 1974), Vol. 4.
[16] P.E. Blöchl, O. Jepsen, and O.K. Andersen, Phys. Rev. B **49**, 16 223 (1994).
[17] M. Kuhn, T.K. Sham, J.M. Chen, and K.H. Tan, Solid State Commun. **75**, 861 (1990).
[18] B. Moraweck, A.J. Renouprez, E.K. Hill, and R. Baudoing-Savois, J. Phys. Chem. **97**, 4288 (1993).
[19] L.V. Azaroff, J. Appl. Phys. **34**, 2809 (1967).
[20] D. C. Koningsberger and R. Prins, *X-ray Absorption* (Wiley, New York, 1988), Chap. 11.
[21] K.H. Chae, Y.S. Lee, S.M. Jung, Y. Jeon, M. Croft, and C.N. Whang, Nucl. Instrum. Methods Phys. Res. B **106**, 60 (1995).
[22] J. Chen, M. Croft, Y. Jeon, X. Xu, S.A. Shaheen, and F. Lu, Phys. Rev. B **46**, 15 639 (1992).
[23] M. Brown, R.E. Peierls, and E.A. Stern, Phys. Rev. B **15**, 738 (1977).
[24] R. F. W. Bader, *Atoms in Molecules—A Quantum Theory* (Oxford University Press, Oxford, UK, 1990).
[25] I.A. Abrikosov, W. Olovsson, and B. Johansson, Phys. Rev. Lett. **87**, 176403 (2001).
[26] W.F. Egelhoff, Jr., Surf. Sci. Rep. **6**, 253 (1987).
[27] F. D. Bloss, *Crystallography and Crystal Chemistry* (Holt, Rinehart and Winston, New York, 1971), p. 194.
[28] W.R.L. Lambrecht, Phys. Rev. B **34**, 7421 (1986).
[29] P.A.P. Nascente, S.G.C. de Castro, R. Landers, and G.G. Kleiman, Phys. Rev. B **43**, 4659 (1991).
[30] J.S. Faulkner, Y. Wang, and G.M. Stocks, Phys. Rev. Lett. **81**, 1905 (1999); R.J. Cole, N.J. Brooks, P. Weightman, and J.A.D. Matthew, Phys. Rev. B **52**, 2976 (1995); T.K. Sham, M.L. Perlman, and R.E. Watson, *ibid.* **19**, 539 (1979); R.E. Watson, M.L. Perlman, and J.F. Herbst, Phys. Rev. B **6**, 2358 (1976); R.E. Watson, J. Hudis, and M.L. Perlman, *ibid.* **4**, 4139 (1971).